Levitation Force on a Permanent Magnet over a Superconducting Plane: Modified Critical-State Model*

by

Z. J. Yang
Argonne National Laboratory
9700 South Cass Avenue
Argonne, IL 60439, USA

*Work at Argonne National Laboratory was performed under the auspices of the U.S. Department of Energy, Energy Efficiency and Renewable Energy, as part of a program to develop electric power technology, under Contract W-31-109-Eng-38.

DISCLAIMER

Levitation Force on a Permanent Magnet over a Superconducting Plane: Modified Critical-State Model

Z.J. Yang

Argonne National Laboratory, Argonne, IL 90439, USA

Abstract

We consider a model system of a permanent magnet above a semi-infinite superconductor. We introduce a modified critical-state model, and carry out derivations of the levitation force acting on the magnet. A key feature of the modification allows the current density to be less than the critical value. The theoretical results show an exponential relationship between the force and the distance. Analytical expressions are developed for permanent magnets in the form of a point dipole, a tip of a magnetic force microscope, and a cylindrical magnet. In the latter case, the exponential relationship has been observed in numerous experiments but without previous interpretation.

PACS numbers: 85.25.-Ly, 41.20.Gz, **74.72.-h**, 61.16.Ch

Keywords: high-Tc superconductor, Meissner effect, critical-state model, magnetic levitation, magnetic force microscope

1 Introduction

With the discovery of high T_c superconductors, magnetic bearings which use these materials have become feasible [1,2]. In this field, many groups reported early experimental investigations [3-8], and a few theoretical papers were also published [9-17].

As far as the theoretical approaches are concerned, there are a numbers of models to evaluate the levitation forces for various configurations [9-17]. Generally, we study the system consisting of a permanent magnet and a (type-II) superconductor. When the magnet is far from the superconductor, the perfect diamagnetic model (assuming the superconductor in complete Meissner state) is fairly good for evaluating the interaction force, because the magnetic induction from the magnet on the superconductor is below the lower critical induction ($< B_{c1}$). However, if the magnet moves closer to the superconductor, the perfect diamagnetic model no longer accurately predicts the levitation force in the system. As a theoretical approach, the London theory of superconductivity was recently employed to derive the forces [11-14]. Extending the aproach based on the London theory, coffey [15] derited a formula of the lifting force acting on a tip of a magnetic force microscope from a vortex in a type-II superconductor. Using the critical-state model, Davis [9] initiated an approach to evaluate the lateral restoring force acting an infinite long current wire above a type-II superconductor. Afterward, Davis' result was extended to some more practical magnets by Yang el al. [16]. However, neither Davis' result nor the extended results could be used to estimate the levitation forces. Using the critical-state models [18, 19], some papers have been published based on the numerical calculations [20]. These numerical calculations are not convenient to see the clear relationships among the physical parameters involved. For instance, it is generally accepted that the levitation forces are basically determined by the critical current density J_c. However, in what kinds of relationships, linear, power-law, and/or other functions, no quantitative expression has been given from these (numerical calculation) papers.

Experiments showed that, as a permanent magnet moves toward a superconductor,

the levitation force is an exponential function of the distance between them (for review, see [3]). However, there is no satisfactory (phenomenological) theory to explain the exponential relationship.

A clear picture of the quantitative description is needed for understanding the physics and applying it to engineering design. In this paper, we introduce a modified critical-state model, and obtain an analytical expression for the relationship between the levitation forces and the current flowing in the superconductor. The model is applied to the derivations of the forces acting on three permanent magnet geometries.

This paper is arranged as follows: The basic equations for a point dipole are given in Section 2. In Section 3, we show the difficulty of using the Bean's critical-state models to derive the levitation forces. The modified critical-state model is introduced, and the relevant derivations for the levitation forces are carried out in Section 4. Discussion is given in Section 5. Section 6 is a short summary.

2 Basic Equations

We consider a (permanent) magnetic dipole with moment $\boldsymbol{m}$ placed at distance a above a semi-infinite superconductor filling the lower half space, as shown in Fig. 1. We consider only the particular configuration, in which the direction of the magnetic moment is along the $z-$axis ($\theta = 0$). From Maxwell's equations, the equations of the vector potential $\boldsymbol{A}(r,z)$ in the free space and the magnetic induction $\boldsymbol{B}(r,z)$ in the superconductor [in the cylindrical coordinates (r,θ,z)] are

$$\nabla^2 \boldsymbol{A}(r,z) = -\mu_0 \nabla \times \boldsymbol{m}\delta(r^2/2)\delta(z-a) \qquad z > 0 \tag{1}$$

$$\nabla \times \boldsymbol{B}(r,z) = \mu_0 \boldsymbol{J}(r,z) \qquad z \leq 0\,, \tag{2}$$

where μ_0 is the vacuum permeability, $\delta(x)$ is the Dirac $\delta-$function, and $\boldsymbol{J}(r,z)$ is the current density. Here, the Coulomb gauge ($\nabla\cdot\boldsymbol{A}=0$) is used in Eq. (1). For Eq. (2), the

vector potential $\boldsymbol{A}(r,z)$ can also be introduced via the general relationship

$$\boldsymbol{B}(r,z) \;=\; \nabla \times \boldsymbol{A}(r,z)\;. \tag{3}$$

Due to the cylindrical symmetry of the system, $\boldsymbol{J}(r,z)$ has only the $\theta-$component, i.e., $\boldsymbol{J}(r,z) = J(r,z)\boldsymbol{e}_\theta$; and the vector potential $\boldsymbol{A}(r,z)$ can be expressed as

$$\boldsymbol{A}(r,z) \;=\; A(r,z)\boldsymbol{e}_\theta \tag{4}$$

with the proper selection of the gauge. Thus, Eqs. (1) and (2) can be simplified to be

$$\left[\frac{1}{r}\frac{\partial}{\partial r}\left(r\frac{\partial}{\partial r}\right) - \frac{1}{r^2} + \frac{\partial^2}{\partial z^2}\right] A(r,z) = \mu_0 m \delta'(r^2/2)\delta(z-a) \qquad z > 0 \tag{5}$$

$$\left[\frac{1}{r}\frac{\partial}{\partial r}\left(r\frac{\partial}{\partial r}\right) - \frac{1}{r^2} + \frac{\partial^2}{\partial z^2}\right] A(r,z) = -\mu_0 J(r,z) \qquad z \le 0\;, \tag{6}$$

where $\delta'(r^2/2) = (\partial/\partial r)\delta(r^2/2)$. Via Eqs. (3) and (4), the magnetic inductions can be derived explicitly by

$$B_r(r,z) \;=\; -\frac{\partial}{\partial z}A(r,z) \tag{7}$$

$$B_z(r,z) \;=\; \frac{1}{r}\frac{\partial}{\partial r}[rA(r,z)]\;. \tag{8}$$

The solutions to Eqs. (5) and (6) can be written in the form

$$A(r,z) = \begin{cases} A_1(r,z) + A_2(r,z) & z > 0 \\ A_3(r,z) + A_4(r,z) & z \le 0 \end{cases} \tag{9}$$

where $A_1(r,z)$ is the direct term (contributed directly from the dipole); $A_2(r,z)$ is the induced term due to the existence of the superconductor; $A_3(r,z)$ is the current term; and the $A_4(r,z)$ is the penetration term. Mathematically, $A_1(r,z)$ and $A_3(r,z)$ are the particular solutions to Eqs. (5) and (6), respectively.

Correspondingly, the magnetic inductions can be expressed in the form

$$\boldsymbol{B}(r,z) = \begin{cases} \boldsymbol{B}_1(r,z) + \boldsymbol{B}_2(r,z) & z > 0 \\ \boldsymbol{B}_3(r,z) + \boldsymbol{B}_4(r,z) & z \le 0 \end{cases} \tag{10}$$

The boundary conditions are given by

$$\boldsymbol{B}_1(r,0^+) + \boldsymbol{B}_2(r,0^+) = \boldsymbol{B}_3(r,0^-) + \boldsymbol{B}_4(r,0^-) \ . \tag{11}$$

The self-interaction energy between the dipole and the superconductor is

$$U(a) \ = \ -\frac{1}{2}\boldsymbol{m}\cdot\boldsymbol{B}_2(0,a) \ . \tag{12}$$

The levitation force acting on the dipole is obtained to be

$$F_z(a) \ = \ -\frac{\partial U(a)}{\partial a} \ . \tag{13}$$

3 Difficulty of the Old Models

In 1960's, Bean introduced the so-called critical-state model to study the magnetization for type-II (or called hard) superconductors [18]. Bean's model was the first successful model to explain the magnetic properties of hard superconductors. However, as shown below, it is difficult to use this model to evaluate the levitation force in the magnet superconductor system.

According to Bean [18], when an external magnetic induction is applied, the supercurrent density $J(r,z)$ is either zero or a critical current density flowing in the superconductor and is a constant, i.e.,

$$J(r,z) = J_{\rm c} = \text{const.} \tag{14}$$

in Eq. (6). Substituting Eq. (14) into Eq. (6), the only particular solution to Eq. (6) is

$$A_3(r,z) = -\frac{1}{3}\mu_0 J_{\rm c} r^2 \ . \tag{15}$$

[Note: It is prerequisite that the solution needs to satisfy Eq. (2) too.]

The magnetic induction has only the $z-$component, which reads

$$B_{3z}(r,z) = -\mu_0 J_{\rm c} r \ . \tag{16}$$

It is easy to see that this solution is non-physical: It is divergent as $r \to \infty$. Similar treatment can be carried out for other critical-state models. None of the available critical-state models [19] provide a convergent solution.

From a mathematical point of view, if $J(r,z)$ is a constant, the corresponding magnetic induction $\boldsymbol{B}_3(r,z)$ must be proportional to $|\boldsymbol{R}|$ [$\boldsymbol{R}= r\boldsymbol{e}_r+(z-a)\boldsymbol{e}_z$], and $A_3(r,z)$ must be proportional to $|\boldsymbol{R}|^2$. No physical solution can be obtained. Furthermore, if $|\boldsymbol{B}_3(r,z)|$ is the order of $|\boldsymbol{R}|^{\epsilon-1}$ ($\epsilon < 1$), $|J(r,z)|$ must be the order of $|\boldsymbol{R}|^{\epsilon-2}$. In fact, all conventional critical-state models do not satisfy these conditions.

In the studies of magnetic properties based on the critical-state models, one very important assumption is that a uniformly external magnetic field is applied to the superconductor sample. However, this condition does not hold at all for the present system. When a dipole (as the external field source) is placed at $(r = 0, z = a)$, the magnetic induction applied to the superconductor is not uniform, but a decreasing function with the power of $|\boldsymbol{R}|^{-3}$ for large $|\boldsymbol{R}|$ from the center $(r = 0, z = a)$. Correspondingly, the amplitude of the magnetic induction $|\boldsymbol{B}_3(r,z)|$ must be a decreasing function of r and z.

Modified critical-state models that fulfil the mathematical and physical restrictions are needed for the investigation of levitation force in the present system with a nonuniform external magnetic field. Modification of the critical-state model can be achieved in several ways. One physical approach is to assume that: (i) There are a series of (cylindrical-symmetrical) critical current loops in the superconductor. (ii) Each of the (critical) current loops has the critical current density J_c, but the loop density (how many loops per unit length) is a decreasing function with increasing r. (iii) All current loops have $r-$dependent cut-off in the z-direction. Due to the nonuniformity of the applied induction from the dipole, the interface (the cut-off function) in the superconductor is very complicated. This complication results in the mathematical difficulty, which is almost impossible to overcome for obtaining an analytical solution. As an alternative approach, we consider continuous decreasing functions to model the current. With this approximation, analytical solutions

of the levitation forces are obtained and provide agreement with experimental data.

4 Modified Critical-State Model

In order to obtain a convergent solution to Eq. (6), we need to modify the current density term [the RHS of Eq. (6)]. It is informative to look at the formula of the current circulating in the superconductor obtained from other theoretical approaches.

Previously, using the London theory of superconductivity we introduced a theoretical approach to estimate the levitation force for the same kind of problem treated here [11, 14]. The current density from the London model reads

$$J_{\rm London}(r,z) \;=\; \frac{m}{4\pi\lambda}\int_0^\infty {\rm d}k \frac{2k^2\ J_1(kr)}{\sqrt{1+k^2\lambda^2}+k\lambda}\ \exp\left(-ka+\sqrt{1+k^2\lambda^2}\ z/\lambda\right)\ , \quad (17)$$

where λ is the effective penetration depth. Here, the basic (self-consistent) solution is $\exp\left(\sqrt{1+k^2\lambda^2}\ z/\lambda\right)J_1(kr)$, where $J_1(x)$ is the 1st-order Bessel function of the first kind.

One may show that the basic solution to the homogeneous equation of Eq. (6) is $e^{kz}J_1(kr)$. [It would be much clearer after reading Appendix A]. The current is a responding current, no matter what models are used in theoretical derivations. From a physical point of view, we could use a function in a similar form as the basic solution to simulate the current density in the critical-state. To modify the basic solution $e^{kz}J_1(kr)$, we can realize it by two ways: to modify the radial part $J_1(kr)$ and/or to reform the vertical part e^{kz}. For simplicity, in this section, we introduce the basic model. A more complicated model and relevant derivations are given in appendices.

Hinted from the results of the London model, for our basic modified critical-state model we consider the current density

$$J(r,z) = -J_{\rm c}\ e^{K_z(z-a)}J_1(K_r r)\ . \quad (18)$$

where $J_{\rm c}$ is the maximum current density in the superconductor, and K_z^{-1} and K_r^{-1} have the length dimensions. In the following derivations, $J_{\rm c}$ is assumed to be a constant

determined by the materials. K_z^{-1} is a measure of the depth in the $z-$direction the current flows in the superconductor, and K_r^{-1} is a measure of the range along the $r-$direction.

In the following three subsections, we present the derivattions of the levitation forces for three typical geometries: point dipole, a pair of magnetic charges (model for a tip of the magnetic force micrroscope), and a cylindrical permanent magnet.

4.1 Point Dipole

For a point dipole above a type-II superconductor as illustrated in Fig. 1 with $\theta = 0$, we consider Eq. (18) decribing the supper-current flowing in the superconductor. For simplicity, we choose $K_z = K_r = K$ in this subsection.

Substituting Eq. (18) into (6), we solve Eqs. (5), (6) and (11). The solutions are

$$A_1(r,z) = \frac{\mu_0 m}{4\pi} \frac{r}{[r^2+(z-a)^2]^{3/2}} \tag{19}$$

$$A_2(r,z) = -\frac{\mu_0 J_c}{4K^2} e^{-K(z+a)}\ J_1(Kr) \tag{20}$$

$$A_3(r,z) = \frac{\mu_0 J_c}{2K^2}(1+Kz)e^{K(z-a)}\ J_1(Kr) \tag{21}$$

$$A_4(r,z) = \frac{\mu_0 m}{4\pi} \frac{r}{[r^2+(z-a)^2]^{3/2}} - \frac{3\mu_0 J_c}{4K^2} e^{K(z-a)}\ J_1(Kr)\ . \tag{22}$$

Using Eqs. (7) and (8), magnetic inductions are

$$B_{1r}(r,z) = \frac{\mu_0 m}{4\pi} \frac{3r(z-a)}{[r^2+(z-a)^2]^{5/2}} \tag{23}$$

$$B_{1z}(r,z) = \frac{\mu_0 m}{4\pi} \frac{2(z-a)^2-r^2}{[r^2+(z-a)^2]^{5/2}} \tag{24}$$

$$B_{2r}(r,z) = -\frac{\mu_0 J_c}{4K} e^{-K(z+a)}\ J_1(Kr) \tag{25}$$

$$B_{2z}(r,z) = -\frac{\mu_0 J_c}{4K} e^{-K(z+a)}\ J_0(Kr) \tag{26}$$

$$B_{3r}(r,z) = -\frac{\mu_0 J_c}{2K}(2+Kz)e^{K(z-a)}\ J_1(Kr) \tag{27}$$

$$B_{3z}(r,z) = \frac{\mu_0 J_c}{2K}(1+Kz)e^{K(z-a)}\ J_0(Kr) \tag{28}$$

$$B_{4r}(r,z) = \frac{\mu_0 m}{4\pi} \frac{3r(z-a)}{[r^2+(z-a)^2]^{5/2}} + \frac{3\mu_0 J_c}{4K} e^{K(z-a)}\ J_1(Kr) \tag{29}$$

$$B_{4z}(r,z) = \frac{\mu_0 m}{4\pi} \frac{2(z-a)^2-r^2}{[r^2+(z-a)^2]^{5/2}} - \frac{3\mu_0 J_c}{4K} e^{K(z-a)}\ J_0(Kr)\ . \tag{30}$$

Using Eqs. (12) and (26) the self-interaction energy is

$$U(a) = \frac{\mu_0 m J_c}{8K} e^{-2Ka} . \quad (31)$$

Using Eq. (13) the levitation force is

$$F_z(a) = \frac{\mu_0 m J_c}{4} e^{-2Ka} . \quad (32)$$

4.2 Tip of the MFM

The magnetic force microscope (MFM) [21] is a powerful tool to probe the magnetic defects in a material. We present a derivation of the lifting force acting on a straight (wire/line) tip of the MFM from a superconducting plane. For simplicity, we model the tip as a long straight wire/line magnet (dipole wire) with a length of l polarized along the line direction. The magnetic induction from the dipole wire is equivalent to the induction from a pair of magnetic charges located at $(0, a)$ and $(0, a + l)$, respectively as illustrated in Fig. 2. For the sake of convenience, we can use the scalar potential method to solve the magnetic induction for the upper space $z > 0$. Eq. (5) is thus replaced by the scalar potential equation

$$\left[\frac{1}{r}\frac{\partial}{\partial r}\left(r\frac{\partial}{\partial r}\right) + \frac{\partial^2}{\partial z^2}\right] V(r,z) = -\mu_0 q\delta(r)\delta(z-a) + \mu_0 q\delta(r)\delta(z-a-l) , \quad (33)$$

where q is the magnetic charge, the moment density per unit length. The magnetic induction can be obtained by

$$\boldsymbol{B}(r,z) = -\nabla V(r,z) . \quad (34)$$

Equation (10) does still hold for the problem. Now, the problem is to solve Eqs. (6) and (33) with boundary condition (11).

Because the sources are a pair of charges, correspondingly, Eq. (18) is replaced by

$$J(r,z) = -J_c\, e^{K_z(z-a)}(1 - e^{-K_z l}) J_1(K_r r) . \quad (35)$$

Using this current density formula with $K_r = K_z = K$, the $z-$component of the induced magnetic flux density is obtained to be

$$B_{2z}(r,z) = -\frac{\mu_0 J_c}{4K} e^{-K(z+a)}(1-e^{-Kl})J_0(Kr) . \quad (36)$$

The self-interaction energy is obtained by integrating over the length of the tip

$$\begin{aligned} U(a) &= \frac{\mu_0 q J_c}{8K^2} e^{-2Ka}(1-e^{-Kl})^2 \\ &\approx \frac{\mu_0 q J_c}{8K^2} e^{-2Ka} . \end{aligned} \quad (37)$$

Here, $Kl >> 1$ was used in the last step.

The levitation force is

$$F_z(a) = \frac{\mu_0 q J_c}{4K} e^{-2Ka} . \quad (38)$$

4.3 Cylindrical Magnet

Let us consider a more practical problem: a cylindrical permanent magnet with radius c, height l, and uniform magnetization $\boldsymbol{M}$ along the $z-$direction over a semi-infinite superconductor, as shown in Fig. 3. Physically, the magnetic induction around the cylinder is equal to the induction from a pair of magnetic charged-disks with radius c and charge density M (per unit area). The centers of the charged-disks are $(0,a)$ and $(0,a+l)$, respectively. Similar to above treatment for the tip of MFM, the direct induction, which is only determined by the source, can be derived from the scalar potential $V_1(r,z)$, which reads

$$\begin{aligned} V_1(r,z) &= \frac{\mu_0 M}{4\pi}\int_0^c \mathrm{d}r'\, r' \int_0^{2\pi} \mathrm{d}\theta \left[\frac{1}{\sqrt{r^2+r'^2-2rr'\cos\theta+(z-a)^2}}\right. \\ &\quad \left. -\frac{1}{\sqrt{r^2+r'^2-2rr'\cos\theta+(z-a-l)^2}}\right] \\ &= \frac{\mu_0 M c}{2}\int_0^\infty \mathrm{d}k\; k^{-1}\, J_1(kc)J_0(kr)\left(e^{-k|z-a|}-e^{-k|z-a-l|}\right) . \end{aligned} \quad (39)$$

Using (34), the direct magnetic induction is obtained to be

$$B_{1r} = \frac{\mu_0 Mc}{2}\int_0^\infty \mathrm{d}k\ J_1(kc)J_1(kr)\left(e^{-k|z-a|}-e^{-k|z-a-l|}\right) \quad (40)$$

$$B_{1z} = \frac{\mu_0 Mc}{2}\int_0^\infty \mathrm{d}k\ J_1(kc)J_0(kr)\left[\mathrm{sgn}(z-a)e^{-k|z-a|}-\mathrm{sgn}(z-a-l)e^{-k|z-a-l|}\right] \quad (41)$$

For the source of a pair of charged-disks, correspondingly, Eq. (18) is replaced by

$$J(r,z) = -J_{\mathrm{c}}\ e^{K_z(z-a)}(1-e^{-K_z l})f(r)\ . \quad (42)$$

where the amplitude of function $f(r)$ is a decreasing function of r for large r. Physically, $f(r)$ should reflect the effect of the radius of the cylindrical magnet. For simplicity, we let $f(r) = J_1(K_r r)$ in this paper.

When the radius of the cylindrical magnet is large, it is reasonable to assume $K_r \neq K_z$ in Eq. (42). (Note: for $K_r = K_z = K$, the derivation are given in Appendix C.) The magnetic inductions are obtained to be

$$B_{2r}(r,z) = -\frac{\mu_0 J_{\mathrm{c}}}{2(K_r+K_z)}e^{-(K_z a+K_r z)}\ J_1(K_r r)(1-e^{-K_z l}) \quad (43)$$

$$B_{2z}(r,z) = -\frac{\mu_0 J_{\mathrm{c}}}{2(K_r+K_z)}e^{-(K_z a+K_r z)}\ J_0(K_r r)(1-e^{-K_z l}) \quad (44)$$

$$B_{3r}(r,z) = \frac{\mu_0 J_{\mathrm{c}} K_z}{K_r^2-K_z^2}e^{K_z(z-a)}\ J_1(K_r r)(1-e^{-K_z l}) \quad (45)$$

$$B_{3z}(r,z) = -\frac{\mu_0 J_{\mathrm{c}} K_r}{K_r^2-K_z^2}e^{K_z(z-a)}\ J_0(K_r r)(1-e^{-K_z l}) \quad (46)$$

$$B_{4r}(r,z) = \frac{\mu_0 Mc}{2}\int_0^\infty \mathrm{d}k\ J_1(kc)J_1(kr)\ e^{k(z-a)}(1-e^{-kl}) - \frac{\mu_0 J_{\mathrm{c}}}{2(K_r-K_z)}e^{K_r z-K_z a}\ J_1(K_r r)(1-e^{-K_z l}) \quad (47)$$

$$B_{4z}(r,z) = -\frac{\mu_0 Mc}{2}\int_0^\infty \mathrm{d}k\ J_1(kc)J_0(kr)e^{k(z-a)}(1-e^{-kl}) + \frac{\mu_0 J_{\mathrm{c}}}{2(K_r-K_z)}e^{K_r z-K_z a}\ J_0(K_r r)(1-e^{-K_z l})\ . \quad (48)$$

The self-interaction energy is obtained by integrating over the volume of the cylinder

$$\begin{aligned} U(a) &= -\frac{1}{2}\int_a^{a+l}\mathrm{d}z\int_0^c \mathrm{d}r\ r\int_0^{2\pi}\mathrm{d}\phi\ MB_{2z}(r,z) \\ &= \frac{\mu_0 MJ_{\mathrm{c}}}{4(K_r+K_z)}\ e^{-K_z a}(1-e^{-K_z l})\int_a^{a+l}\mathrm{d}z\ e^{-K_r z}\int_0^c \mathrm{d}r\ r\int_0^{2\pi}\mathrm{d}\phi\ J_0(K_r r) \\ &= \frac{\pi\mu_0 McJ_{\mathrm{c}}}{2(K_r+K_z)K_r^2}\ J_1(K_r c)\ e^{-(K_r+K_z)a}(1-e^{-K_r l})(1-e^{-K_z l})\ . \end{aligned} \quad (49)$$

The levitation force is

$$F_z(a) = \frac{\pi\mu_0 McJ_c}{2K_r^2} J_1(K_r c)\, e^{-(K_r+K_z)a}(1-e^{-K_r l})(1-e^{-K_z l}) . \quad (50)$$

We have the formulae for extreme conditions

$$F_z(a) \rightarrow \frac{\pi\mu_0 McJ_c}{2K_r^2} J_1(K_r c)\, e^{-(K_r+K_z)a} \text{ as } l \rightarrow \infty \quad (51)$$

$$F_z(a) \rightarrow \frac{\mu_0 qJ_c}{4K_r} e^{-(K_r+K_z)a} \text{ as } l \rightarrow \infty \text{ and } c \rightarrow 0 , \quad (52)$$

where $q = 2\pi Mc^2$, the magnetic charge (moment density per unit length). These two formulae give the lifting force acting a semi-infite tip of the MFM for $K_r \neq K_z$. Equation (51) is for the cylinder-shaped tip, and Eq. (52) is for the wire/line tip.

The force pressure is

$$P_z(a) = \frac{F_z(a)}{\pi c^2} = \frac{\mu_0 MJ_c}{2K_r^2 c} J_1(K_r c)\, e^{-(K_r+K_z)a}(1-e^{-K_r l})(1-e^{-K_z l}) . \quad (53)$$

When $K_r c << 1$ and $l \rightarrow \infty$, it reduces to

$$P_z(a) \rightarrow \frac{\mu_0 MJ_c}{4K_r} e^{-(K_r+K_z)a} . \quad (54)$$

Physically, for a large cylindrical magnet, the super-current in the superconductor is to maximize at $r = c$, i.e., at the same radius as the Ampèrian current in the magnet. Empirically, one expects this to correspond to the maximum of $J_1(x)$, i.e., $K_r c = 1.84$. Here, the value of K_r is set by the radius of the magnet, i.e., $K_r = 1.84/c$. Thus, the force pressure is proportional to McJ_c. Explicitly, as $l \rightarrow \infty$ and $a \rightarrow 0$, we have

$$P_{\text{PM/HTS}}(a \rightarrow 0, l \rightarrow \infty) \rightarrow 0.172\mu_0 McJ_c . \quad (55)$$

This is in agreement with the experimental observation. It is worthy to compare this result with that between two permanent magnets. If we replace the superconductor by a semi-infinite permanent magnet (PM1) with magnetization M_1 along the $z-$direction, the magnetic induction above the upper surface is

$$B_{\text{PM1}} = \frac{\mu_0 M_1}{2} . \quad (56)$$

The force pressure is

$$P_{\mathrm{PM/PM1}} = \frac{\mu_0 M M_1}{2} . \tag{57}$$

(Note: this result is also valid for two semi-infinite long permanent cylindrical magnets at $a = 0$. See Appendix D for details.) When $0.344 c J_c > M_1$, we expect

$$P_{\mathrm{PM/HTS}} > P_{\mathrm{PM/PM1}}, \text{ as } l \to \infty \text{ and } a \to 0 . \tag{58}$$

For instance, if $\mu_0 M_1 = 1$ T for PM1, thus we have $P_{\mathrm{PM/HTS}} > P_{\mathrm{PM/PM1}}$ when $cJ_c > 2.31 \times 10^6$ A/m. This condition is achievable nowadays via so-called melt-texturred technique. This has very high-valued implication in engineering. If one can make the HTS materials with very high J_c-value, the levitation force from the PM/HTS system might be greater that from the PM/PM1 system.

5 Discussion

The basic model is very simple, and the results, Eqs. (32), (38), and (50), show directly the exponential dependence of levitation on height, in agreement with many experiments. We note that the force at zero height is independent of K. Using a semi-log plot for the measured data, the penetration depth and critical current density can be acquired from the slope and intercept, respectively.

For comparison, two sets of experimental data were presented in Fig. 4. Set 1 data were obtained from a sintered Y123 disk with diameter 7 cm and thickness 7 mm and a cylindrical Nd-Fe-B permanent magnet with height and diameter 5 mm. The moment of the magnet was measured to be 8.59×10^{-2} Am^2. Set 2 data were obtained from a melt-textured Y123 disk with diameter 2.54 cm and thickness 10 mm and a cylindrical Nd-Fe-B permanent magnet with height and diameter 12.7 mm. The moment of the magnet was estimated to be 1.41 Am^2. (Note: that the cylinder is approximated as a sphere is a fairly good approximation for the square cylinder. The field value has less than

10% relative error when the distance from the center of the cylinder is equal to or larger than the height/diameter of the cylinder. The magnetic induction around a spherical magnet is equal to that from a point dipole with the same moment located at the center of the sphere.) Via the semi-log plot, as illustrated in the figure, it is easy to see that both sets of experimental data could reasonably be fitted by the exponential functions. From a mathematical point of view, the theoretical and experimental data can be rescaled into one curve because the two group data have the same curvature in the semi−log (or log−log) plots. The exponential relationships were previously reported by many groups (for review, see [3]). However, to the best of our knowledge, there is no quantitative (phenomenological) theory published to explain the experimental observation. The present work is the first theoretical approach leading to the exponential function.

Using Eq. (32), via rescaling the experimental data, we obtained that $J_c = 2.6 \times 10^2$ A/cm^2 and $1/K = 4.7$ mm for Set 1 data, and $J_c = 1.9 \times 10^4$ A/cm^2 and $1/K = 3.1$ mm for Set 2 data. To illustrate the clarity, Fig. 5 shows the rescaling of the experimental data Set 2 against Eq. (32). It is easy to see the fairness of the rescaling.

If the data set 2 are rescaled to the curve of Eq. (50), the critical current density $J_c = 1.2 \times 10^8$ A/m^2 with choosing $K_r c = 0.5$. (Note: $K_z^{-1} = 4.6$ mm is calculated.)

According to the theory of classical electrodynamics, the interaction energy for a magnetic dipole $\boldsymbol{m}$ in an external magnetic induction $\boldsymbol{B}_{\rm ext}$ is given by

$$U_{\rm int} = -\boldsymbol{m} \cdot \boldsymbol{B}_{\rm ext} . \tag{59}$$

Comparing this equation with Eq. (31), we may see the corresponding relation: $\mu_0 J_c/K \propto |\boldsymbol{B}_{\rm ext}|$. Compared with the Bean's critical-state model [18], it becomes clear that K^{-1} is a measure of depth that the external magnetic induction can penetrate in the superconductor.

Physically, it is standing that the current is exponential decreasing function of z, which is used in this paper. However, it is difficult to simulate the currents along the $r-$direction. Consider the source induction from the dipole, $|\boldsymbol{B}| \propto r^{-3}$ as r is large

enough, it is reasonable to believe that the $r-$part of the function in the basic model [Eq. (18)$\rightarrow r^{-1/2}$ as $r \rightarrow \infty$] is too slowly decreasing. One may see that the super-current in Model-II, given in Appendix A, [Eq. (60)$\rightarrow e^{-K_1 r}$ as $r \rightarrow \infty$] is too fast decreasing. Even so large difference between these two models, the two models could yield good agreement results. This agreement indicates that the $z-$part of the currents plays more fundamental rôle compared with the $r-$part.

It is worthy to compare the present approach with the London model [11, 14]. The London theory gives the power-law (with exponent -2) relationship between the levitation force and the distance as the magnet is close enough to the superconductor. However, the present modified critical-state models yield the exponential dependence of the levitation force on the distance. In the London theory, the current is proportional to the vector potential, and the self-consistent condition is described by the linear relationship. Somehow, in the present model, the linear relationship does not hold, and the e^{-aK} terms are artificially introduced to the current formulae for self-consistent adjustment. This self-consistent adjustment is physically needed due to the non-uniformity of the external field from the dipole. The current density has to change as the external field changes.

It is worthy to point out that the levitation forces are linearly proportional to the critical current density J_c from the present simple model calculations. This linear relationship provides a clear guidance how to achieve higher levitation force through enhancing the critical current density of the levitator. On the other hand, we can make an experimental setup to evaluate the quality of the levitators via measuring the levitation forces.

Similar to the result of the dipole, the lifting force acting on a tip of the MFM, Eq. (38), has two undetermined parameters, J_c and K. Via rescaling the force and distance, it is straightforward to obtained these two parameters. An important implication of the present result [Eq. (38)] is to measure the local distribution of the critical current density J_c by using the MFM. Compared to other electromagnetic measurements, the non-contact MFM technique has many advantages in experiments. In particular, the non-contact

measurement would be very useful for the film specimens, because the contact-resistance is a big trouble-matter for the high-current transportation measurements.

The present theoretical approach has some weakness. First, the demagnetization of the permanent magnet from the induced magnetic flux density is very small for the currently used Nd-Fe-B materials, we assume this effect can be ignored. Second, some results [Eqs. (32), (38), and (50)] are valid only when aK (or aK_z) is small. When the magnet is far away from the superconductor, the magnetic induction applied to the superconductor is weak, the superconductor will not be in the critical-state. Fortunately, we do not need to use the present models to deal with the problem when the magnet is far away from the superconductor (i.e., aK or $aK_z >> 1$), because the perfect diamagnetic model is good enough to study the problem.

6 Summary

In this paper, after presenting the field equations for the magnet superconductor (levitation) system, we generally discussed the possibility to calculate the levitation forces via using the critical-state model. To overcome (or go around) the mathematical difficulty of the Bean's model, a modified critical-state model is introduced for solving the problem when the magnet is close to the superconductor. Using the new model, we showed that (i) the maximal levitation force is linearly depending on the critical current density, (ii) the levitation force is exponentially increasing as the magnet moves closer to the superconductor, which was observed and reported by many research groups without interpretation, and (iii) it is possible that the levitation force between a permanent magnet and an HTS is large than that between two permanent magnets.

Acknowledgements

This work was partially supported by the U.S. Department of Energy, Energy Efficiency and Renewable Energy, as part of a program to develop electric power technology, under

Contract W-31-109-Eng-38. The author would like to thank Dr. J.R. Hull for stimulating discussion, and to thank A. Lockwood for the help in experiments [for acquiring Set 2 data in Fig. 4].

Appendix A, Model-II

Similar to the basic model Eq. (18), we consider a more complicated function to simulate the current density

$$J(r,z) = J_{c1}\, e^{K_\perp(z-a-r)} \left[J_0(K_\parallel r) - \frac{2}{3} J_1(K_\parallel r) - \frac{1}{3} J_2(K_\parallel r) \right] , \tag{60}$$

where J_{c1} has the same physical meaning as J_c in the basic model, $K_\parallel^{-1}$ and $K_\perp^{-1}$ have the same physical meanings as K_r^{-1} and K_z^{-1} in the basic model. Here, $J_\nu(x)$ are the ν'th-order Bessel functions of the first kind.

Here, we take $K_\parallel = K_\perp = K_1$ for convenience. The solutions to Eqs. (5) and (6) can thus be expressed in the form

$$\begin{aligned}
A_1(r,z) &= \frac{\mu_0 m}{4\pi} \frac{r}{[r^2+(z-a)^2]^{3/2}} \\
A_2(r,z) &= \frac{\mu_0 m}{4\pi} \int_0^\infty \mathrm{d}k\, C_2(k)\, e^{-k(z+a)} J_1(kr) \qquad (61) \\
A_3(r,z) &= -\frac{2\mu_0 J_{c1}}{3K_1^2} e^{K_1(z-a-r)} J_1(K_1 r) \qquad (62) \\
A_4(r,z) &= \frac{\mu_0 m}{4\pi} \int_0^\infty \mathrm{d}k\, C_4(k)\, e^{k(z-a)} J_1(kr) \, . \qquad (63)
\end{aligned}$$

Using Eqs. (7) and (8), magnetic inductions can be obtained to be

$$\begin{aligned}
B_{1r}(r,z) &= \frac{\mu_0 m}{4\pi} \frac{3r(z-a)}{[r^2+(z-a)^2]^{5/2}} \\
B_{1z}(r,z) &= \frac{\mu_0 m}{4\pi} \frac{2(z-a)^2 - r^2}{[r^2+(z-a)^2]^{5/2}} \\
B_{2r}(r,z) &= \frac{\mu_0 m}{4\pi} \int_0^\infty \mathrm{d}k\, C_2(k) k\, e^{-k(z+a)} J_1(kr) \qquad (64) \\
B_{2z}(r,z) &= \frac{\mu_0 m}{4\pi} \int_0^\infty \mathrm{d}k\, C_2(k) k\, e^{-k(z+a)} J_0(kr) \qquad (65) \\
B_{3r}(r,z) &= \frac{2\mu_0 J_{c1}}{3K_1} e^{K_1(z-a-r)} J_1(K_1 r) \qquad (66)
\end{aligned}$$

$$B_{3z}(r,z) = \frac{2\mu_0 J_{c1}}{3K_1} e^{K_1(z-a-r)} \left[J_1(K_1 r) - J_0(K_1 r)\right] \quad (67)$$

$$B_{4r}(r,z) = -\frac{\mu_0 m}{4\pi} \int_0^\infty \mathrm{d}k\, C_4(k) k\; e^{k(z-a)} J_1(kr) \quad (68)$$

$$B_{4z}(r,z) = \frac{\mu_0 m}{4\pi} \int_0^\infty \mathrm{d}k\, C_4(k) k\; e^{k(z-a)} J_0(kr)\ . \quad (69)$$

Using Eq. (11), the coefficient functions $C_2(k)$ and $C_4(k)$ can be determined to be

$$C_2(k) = \frac{4\pi J_{c1}}{3mK_1} \left[I_2(k,K_1) - I_1(k,K_1)\right] e^{(k-K_1)a} \quad (70)$$

$$C_4(k) = k + \frac{4\pi J_{c1}}{3mK_1} \left[I_2(k,K_1) + I_1(k,K_1)\right] e^{(k-K_1)a}\ , \quad (71)$$

where

$$I_1(k,K_1) = \int_0^\infty \mathrm{d}r\, r\; e^{-K_1 r} J_0(kr) \left[J_0(K_1 r) - J_1(K_1 r)\right] \quad (72)$$

$$I_2(k,K_1) = \int_0^\infty \mathrm{d}r\, r\; e^{-K_1 r} J_1(kr) J_1(K_1 r)\ . \quad (73)$$

The self-interaction energy is

$$\begin{aligned} U(a) &= -\frac{\mu_0 m^2}{8\pi} \int_0^\infty \mathrm{d}k\, C_2(k) k\; e^{-2ka} \\ &= -\frac{\mu_0 m J_{c1}}{6K_1} e^{-K_1 a} \int_0^\infty \mathrm{d}k\, k\; e^{-ka} \int_0^\infty \mathrm{d}r\, r\, e^{-K_1 r} \\ &\quad \times \left\{J_1(kr) J_1(K_1 r) - J_0(kr) \left[J_0(K_1 r) - J_1(K_1 r)\right]\right\} \\ &= -\frac{\mu_0 m J_{c1}}{6K_1} e^{-K_1 a} \int_0^\infty \mathrm{d}r\, r\, e^{-Kr} \frac{(a+r) J_1(K_1 r) - a J_0(K_1 r)}{(r^2+a^2)^{3/2}}\ . \end{aligned} \quad (74)$$

The levitation force is

$$\begin{aligned} F_z(a) &= \frac{\mu_0 m J_{c1}}{6K_1} e^{-K_1 a} \int_0^\infty \frac{\mathrm{d}r\, r\, e^{-K_1 r}}{(r^2+a^2)^{5/2}} \Big\{\left[2a^2 - r^2 + K_1 a(a^2+r^2)\right] J_0(K_1 r) \\ &\quad + \left[r^2 - 2a^2 - 3ar + K_1(a+r)(a^2+r^2)\right] J_1(K_1 r)\Big\}\ . \end{aligned} \quad (75)$$

To visualize the relationship between the levitation force and distance for Model-II, we plot [Eq. (75)] the force (in units of $\mu_0 m J_{c1}/6$) as a function of a (in units of $1/K_1$) in Fig. 6(a). As illustrated in the figure, in the range of practical experimental measurements, the levitation force can reasonably be fitted as an exponential function of the distance.

Using (75), via rescaling the experimental data shown in Fig. 4, we obtained that $J_{c1} = 2.9 \times 10^2$ A/cm^2 and $1/K = 4.6$ mm for Set 1 data, and $J_{c1} = 2.1 \times 10^4$ A/cm^2 and

$1/K = 2.9$ mm for Set 2 data. These data are in good agreement with those obtained via the basic model.

Appendix B, Model-II for tip of the MFM

Similar to the treatment in Section 4.2, Eq. (60) is replaced by

$$J(r,z) = J_{c1}\, e^{K_\perp(z-a-r)}(1-e^{-K_\perp l})\left[J_0(K_\parallel r) - \frac{2}{3}J_1(K_\parallel r) - \frac{1}{3}J_2(K_\parallel r)\right] , \qquad (76)$$

Using this formula with $K_\parallel = K_\perp = K_1$, the $z-$component of the induced magnetic flux density is obtained to be

$$B_{2z}(r,z) = \frac{\mu_0 J_{c1}}{3K_1} e^{-K_1 a}(1-e^{-K_1 l}) \int_0^\infty \mathrm{d}k\, k\; e^{-kz}\, J_0(kr)\left[I_2(k,K_1) - I_1(k,K_1)\right] , \qquad (77)$$

where $I_1(k,K_1)$ and $I_2(k,K_1)$ are defined by Eqs. (72) and (73).

The interaction between the tip and the superconducting plane is

$$\begin{aligned} U(a) &= -\frac{\mu_0 q J_{c1}}{6K_1} e^{-K_1 a}(1-e^{-K_1 l}) \int_0^\infty \mathrm{d}r\, e^{-K_1 r}\left\{ J_1(K_1 r)\left[\frac{a+l-r}{\sqrt{r^2+(a+l)^2}} - \frac{a-r}{\sqrt{r^2+a^2}}\right]\right. \\ &\quad \left. + J_0(K_1 r)\left[\frac{r}{\sqrt{r^2+(a+l)^2}} - \frac{r}{\sqrt{r^2+a^2}}\right]\right\} \\ &\approx \frac{\mu_0 q J_{c1}}{6K_1} e^{-K_1 a} \int_0^\infty \mathrm{d}r\, \frac{r J_0(K_1 r) + (a-r) J_1(K_1 r)}{\sqrt{r^2+a^2}}\, e^{-K_1 r} . \end{aligned} \qquad (78)$$

The approximation $a << l$ was used in the last step.

The lifting force acting on the tip is obtained to be

$$\begin{aligned} F_z(a) &= \frac{\mu_0 q J_{c1}}{6K_1} e^{-K_1 a} \int_0^\infty \frac{\mathrm{d}r\, e^{-K_1 r}}{(r^2+a^2)^{3/2}} \left\{[ar + K_1 r(a^2+r^2)] J_0(K_1 r)\right. \\ &\quad \left. - [(a+r)r - K_1(a-r)(a^2+r^2)] J_1(K_1 r)\right\} . \end{aligned} \qquad (79)$$

To visualize the relationship in Model-II, Eq. (79), the force (in units of $\mu_0 m J_{c1}/6K_1$) as a function of a (in units of $1/K_1$), is plotted in Fig. 6(b). As illustrated in the figure, it is easy to see that the force is an exponential function of aK_1 in the range of experimental interest.

Appendix C, Cylindrical Magnet for $K_r = K_z = K$

Using Eq. (39) with $K_r = K_z = K$, we obtain the magnetic inductions as

$$
\begin{aligned}
B_{2r}(r,z) &= -\frac{\mu_0 J_c}{4K} e^{-K(z+a)}\, J_1(Kr)(1-e^{-Kl}) && (80)\\
B_{2z}(r,z) &= -\frac{\mu_0 J_c}{4K} e^{-K(z+a)}\, J_0(Kr)(1-e^{-Kl}) && (81)\\
B_{3r}(r,z) &= -\frac{\mu_0 J_c}{2K}(2+Kz) e^{K(z-a)}\, J_1(Kr)(1-e^{-Kl}) && (82)\\
B_{3z}(r,z) &= \frac{\mu_0 J_c}{2K}(1+Kz) e^{K(z-a)}\, J_0(Kr)(1-e^{-Kl}) && (83)\\
B_{4r}(r,z) &= \frac{\mu_0 Mc}{2}\int_0^\infty \mathrm{d}k\; J_1(kc)J_1(kr)e^{k(z-a)}(1-e^{-kl})\\
&\quad + \frac{3\mu_0 J_c}{4K} e^{K(z-a)}\, J_1(Kr)(1-e^{-Kl}) && (84)\\
B_{4z}(r,z) &= -\frac{\mu_0 Mc}{2}\int_0^\infty \mathrm{d}k\; J_1(kc)J_0(kr)e^{k(z-a)}(1-e^{-kl})\\
&\quad - \frac{3\mu_0 J_c}{4K} e^{K(z-a)}\, J_0(Kr)(1-e^{-Kl})\,. && (85)
\end{aligned}
$$

The self-interaction energy is obtained by integrating over the volume of the cylinder

$$
\begin{aligned}
U(a) &= -\frac{1}{2}\int_a^{a+l}\mathrm{d}z\int_0^c \mathrm{d}r\; r\int_0^{2\pi}\mathrm{d}\phi\; MB_{2z}(r,z)\\
&= \frac{\mu_0 M J_c}{8K}\, e^{-Ka}(1-e^{-Kl})\int_a^{a+l}\mathrm{d}z\; e^{-Kz}\int_0^c \mathrm{d}r\; r\int_0^{2\pi}\mathrm{d}\phi\; J_0(Kr)\\
&= \frac{\pi\mu_0 McJ_c}{4K^3}\, J_1(Kc)\; e^{-2Ka}(1-e^{-Kl})^2\,. && (86)
\end{aligned}
$$

The levitation force is

$$
F_z(a) = \frac{\pi\mu_0 McJ_c}{2K^2}\, J_1(Kc)\; e^{-2Ka}(1-e^{-Kl})^2\,. \qquad (87)
$$

When $Kl >> 1$ and very small Kc, we have $q = M\pi c^2$ and $J_1(x) \approx x/2$, and thus, this result reduces to Eq. (38).

The force pressure is

$$
P_z(a) = \frac{F_z(a)}{\pi c^2} = \frac{\mu_0 MJ_c}{2K^2 c}\, J_1(Kc)\; e^{-2Ka}(1-e^{-Kl})^2\,. \qquad (88)
$$

Appendix D, Two Permanent Cylindrical Magnets

Consider two semi-infinite long permanent cylindrical magnets aligned symmettrically as shown in Fig. 7. The magnetizations are $\boldsymbol{M}$ and $\boldsymbol{M}_1$, respectively. The radii are c and c_1. Without loss of generality, let $c_1 > c$.

From Section 4.2, we know that the $z-$component of the magnetic induction from the lower magnet is

$$B_{1z} = \frac{\mu_0 M_1 c_1}{2} \mathrm{sgn}(z) \int_0^\infty \mathrm{d}k \; J_1(kc_1) J_0(kr) e^{-kz} \; . \tag{89}$$

The $z-$component of the levitation force acting the upper magnet is

$$\begin{aligned} F_z(a) &= \frac{\mu_0 M M_1 c_1}{2} \int_0^\infty \mathrm{d}k \; J_1(kc_1) \int_0^c \mathrm{d}r \; r \int_0^{2\pi} \mathrm{d}\theta \; J_0(kr) e^{-ka} \\ &= \mu_0 \pi M M_1 c c_1 \int_0^\infty \mathrm{d}k \; k^{-1} \; J_1(kc) J_1(kc_1) e^{-ka} \; . \end{aligned} \tag{90}$$

When $a = 0$, we have

$$F_z(a=0) = \frac{\mu_0 \pi M M_1 c^2}{2} \; . \tag{91}$$

The force pressure is

$$P(a=0) = \frac{F_z(a=0)}{\pi c^2} = \frac{\mu_0 M M_1}{2} \; . \tag{92}$$

References

[1] F.C. Moon, *Nature*, **350** 270 (1991).

[2] Z.J. Yang, Ph.D. Thesis, University of Oslo (1991).

[3] F.C. Moon, *Superconducting Levitation*, (Wiley, New York, 1994).

[4] P.-Z. Chang, F.C. Moon, J.R. Hull and T.M. Mulcahy, *J. Appl. Phys.* **67** 4358 (1990).

[5] B.R. Weinberger, L. Lynds, and J.R. Hull, *Supercond. Sci. Technol.* **3** 381 (1990).

[6] D.B. Marshall, R.E. DeWames, P.E.D. Morgan and J.J. Ratto, *Appl. Phys.* **A 50** 445 (1990).

[7] Y. Shapira, C.Y. Huang, E.J. McNiff Jr, P.N. Peters, B.B. Schwartz and M.K. Wu, *J. Magn. & Magn. Mater.* **78** 19 (1989).

[8] Z.J. Yang, T.H. Johansen, H. Bratsberg, G. Helgesen and A.T. Skjeltorp, *Physica* **C160** 461 (1989).

[9] L.C. Davis, *J. Appl. Phys.* **67** 2631 (1990).

[10] L.C. Davis, E.M. Logothetis and R.E. Soltis, *J. Appl. Phys.* **64** 4212 (1988).

[11] Z.J. Yang, *Jpn. J. Appl. Phys.* **31** L477 (1992).

[12] Z.J. Yang, *J. Supercond.* **5** 259 (1992).

[13] Z.J. Yang, *Jpn. J. Appl. Phys.* **31** L938 (1992).

[14] Z.J. Yang, T.H. Johansen, H. Bratsberg, A. Bhatnagar, and A.T. Skjeltorp, *Physica* **C 197** 136 (1992).

[15] M. W. Coffey, *Phys. Rev.* **B** in press (1995).

[16] Z.J. Yang, T.H. Johansen, H. Bratsberg, G. Helgesen, and A.T. Skjeltorp, *J. Appl. Phys.* **68** 3761 (1990).

[17] Z.J. Yang, *Appl. Supercond.* **2** 559 (1994).

[18] C.P. Bean, *Rev. Mod. Phys.*, **36** 31 (1964).

[19] M. Xu, D.L. Shi, and R.F. Fox, *Phys. Rev.*, **B42** 10773 (1990).

[20] T.H. Johansen and H. Bratsberg, *J. Appl. Phys.*, **74** 4060 (1993), W.C. Chan, D.S. Jwo, Y.F. Lin, and Y. Huang, *Physica*, **C 230** 349 (1994), Y. Yoshida, M. Uesaka, K. Miya, *Int. J. Appl. Electromagnet. Mater.*, **5** 83 (1994).

[21] D. Rugar, H.J. Martin, P. Güthner, P. Lambert, J.E. Stern, I. McFadyen, and T. Yogi, *J. Appl. Phys.* **68** 1169 (1990).

Figure Captions

Fig. 1. Diagram of magnetic dipole ($\boldsymbol{m}$) placed above semi-infinite superconductor.

Fig. 2. Diagram of long wire/line tip of magnetic force microscope placed above semi-infinite superconductor.

Fig. 3. Diagram of cylindrical permanent magnet with magnetization $\boldsymbol{M}$, radius c, and height l placed above semi-infinite superconductor.

Fig. 4. Two sets of the experimental data. The parameters of experiments are: $m = 8.59 \times 10^{-}2$ Am^2 for Set 1 ($\bullet$, the solid line is the fitted curve via an exponential function), and $m = 1.41$ Am^2 for Set 2 ($\square$, the broken line is the fitted curve via an exponential function). Set 1 data were obtained for a sintered Y123 disk with diameter 7 cm [14], and Set 2 data were obtained for a melt-textured Y123 disk with diameter 2.54 cm.

Fig. 5. Illustration of rescaling experimental data into theoretical curves, Eq. (32), for data Set 2.

Fig. 6. (a): Eq. (75), the levitation force (in units of $\mu_0 m J_{c1}/6$) acting on a magnetic dipole as a function of the distance aK_1 ($\circ$). The fitted exponential function is plotted by the solid line. (b): Eq. (79), the lifting force (in units of $\mu_0 q J_{c1}/6K_1$) acting on a semi-infinitely wire/line tip of the MFM as a function of the distance aK_1 ($\circ$). The fitted exponential function is plotted by the solid line.

Fig. 7. Sideview of two semi-infinite long cylindrical permanent magnets with magnetization $\boldsymbol{M}$ and $\boldsymbol{M}_1$, radii c and c_1.

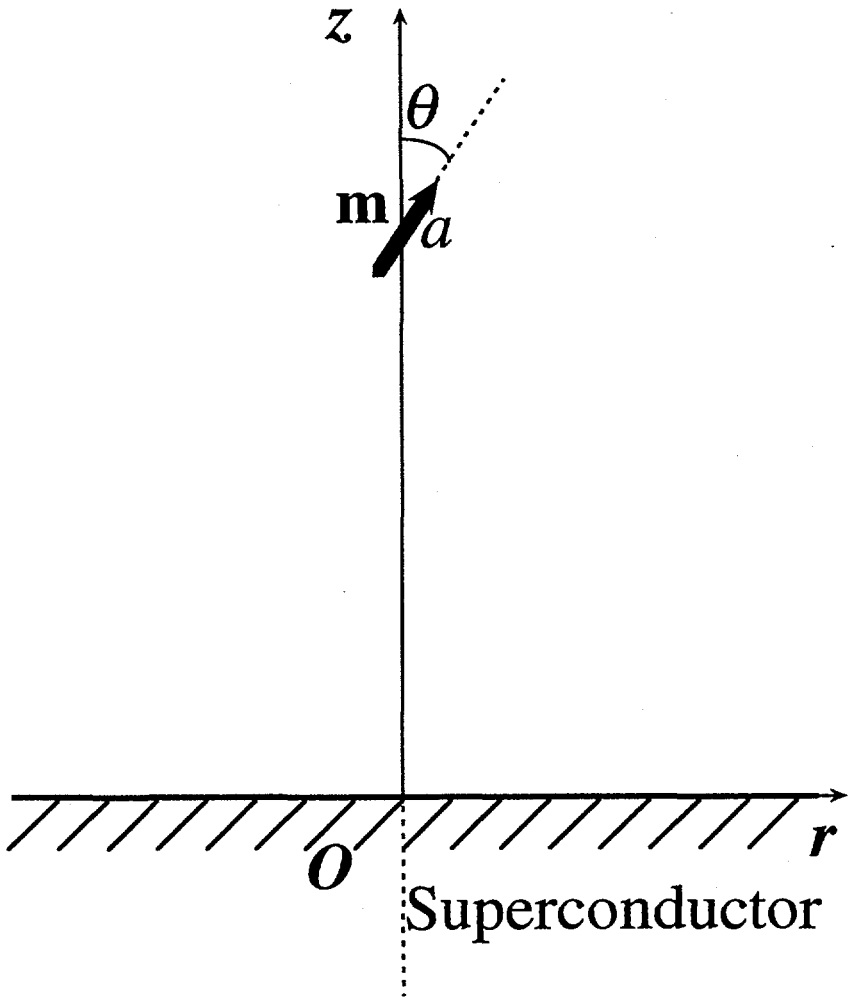

Fig. 1. Z.J. Yang

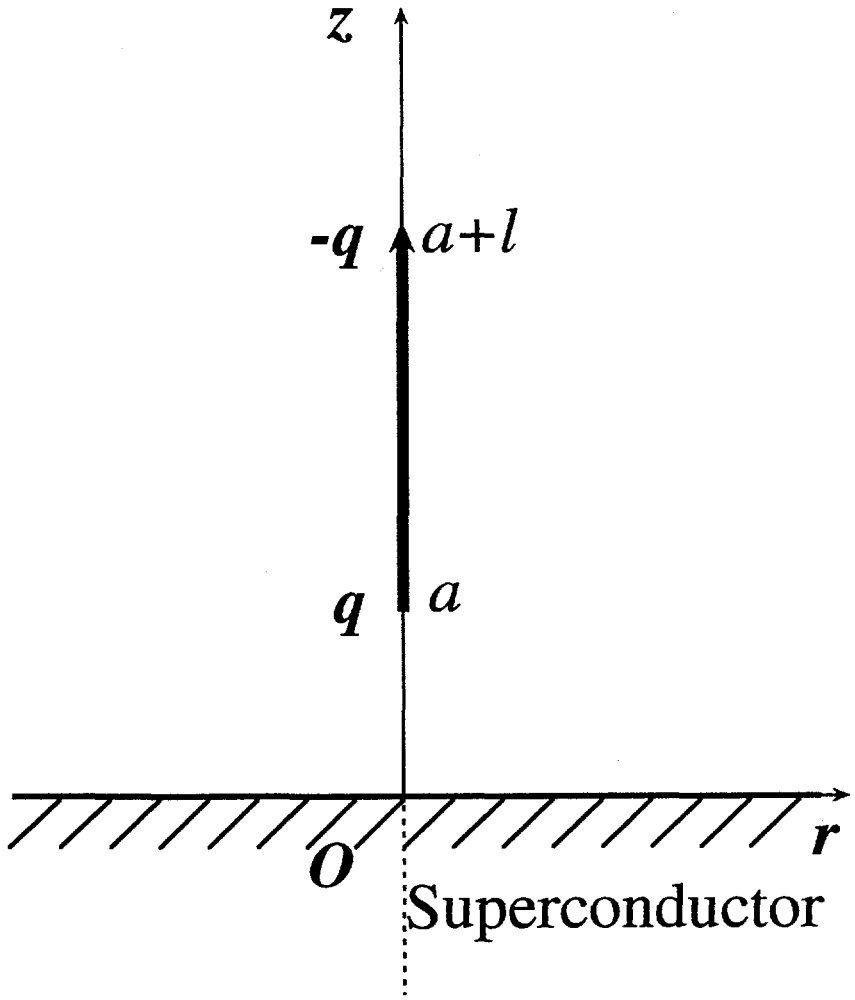

Fig. 2. Z.J. Yang

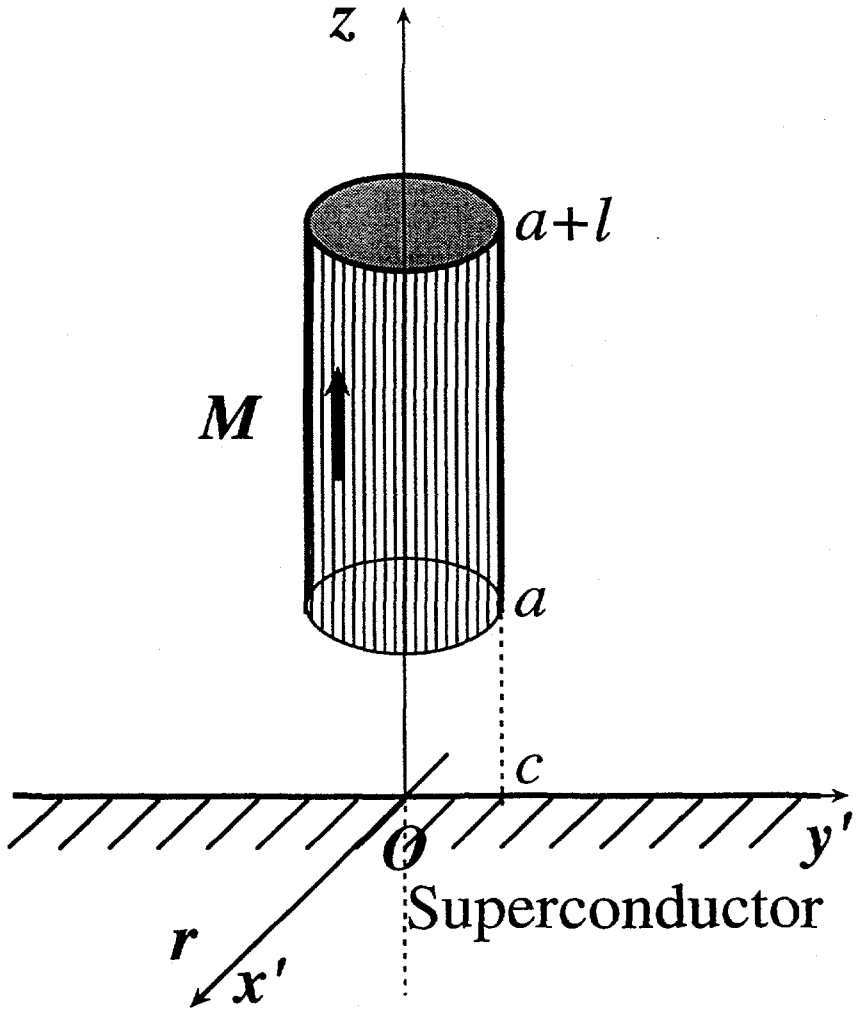

Fig. 3. Z.J. Yang

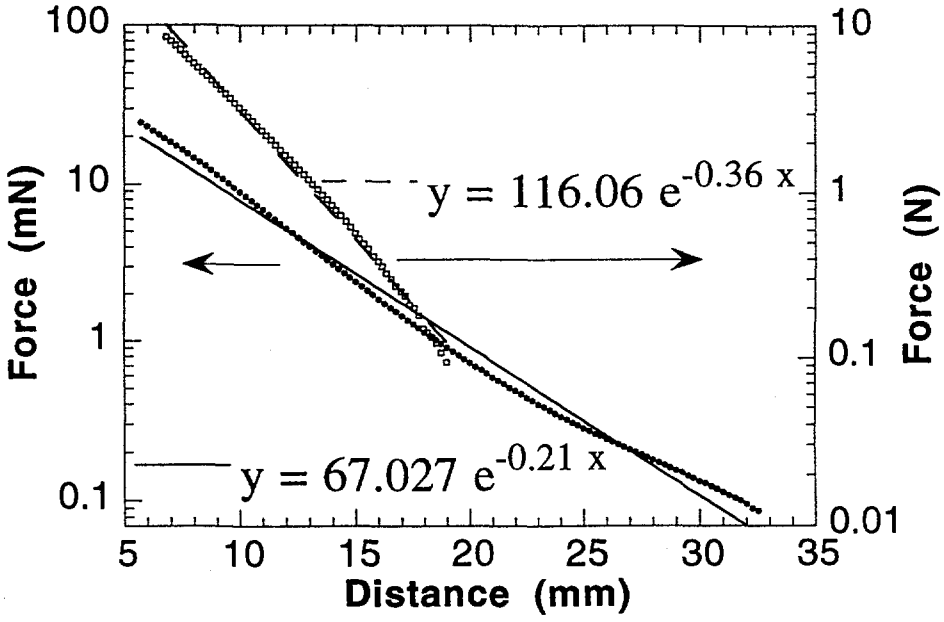
100
10
1
0.1
10
1
0.1
0.01
Force (mN)
Force (N)
y = 116.06 e-0.36 x
y = 67.027 e-0.21 x
5
10
15
20
25
30
35
Distance (mm)

Fig. 4. Z. J. Yang

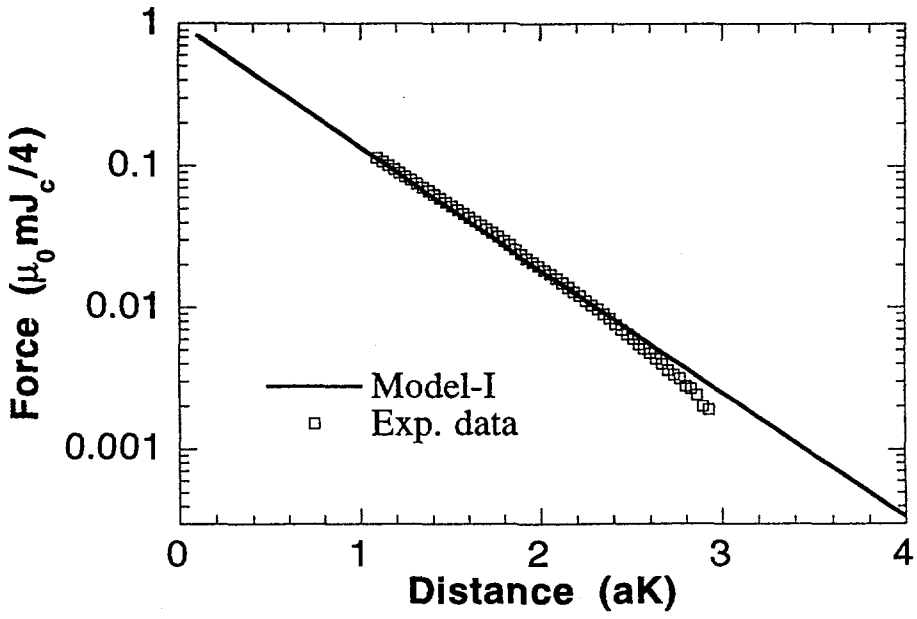
1
0.1
0.01
0.001
Force ($\mu_0 mJ_c/4$)
Model-I
Exp. data
0
1
2
3
4
Distance (aK)

Fig. 5. Z. J. Yang

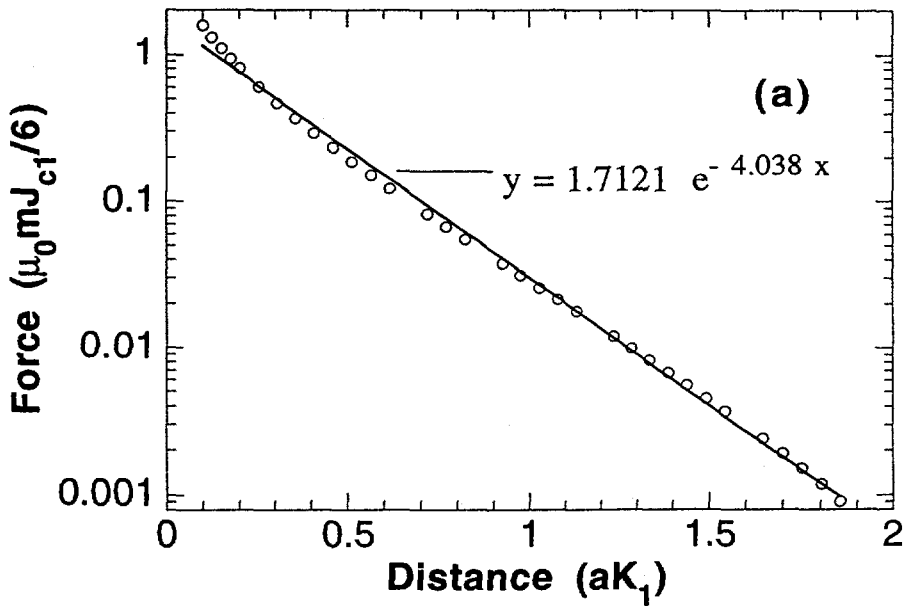

Fig. 6(a). Z. J. Yang

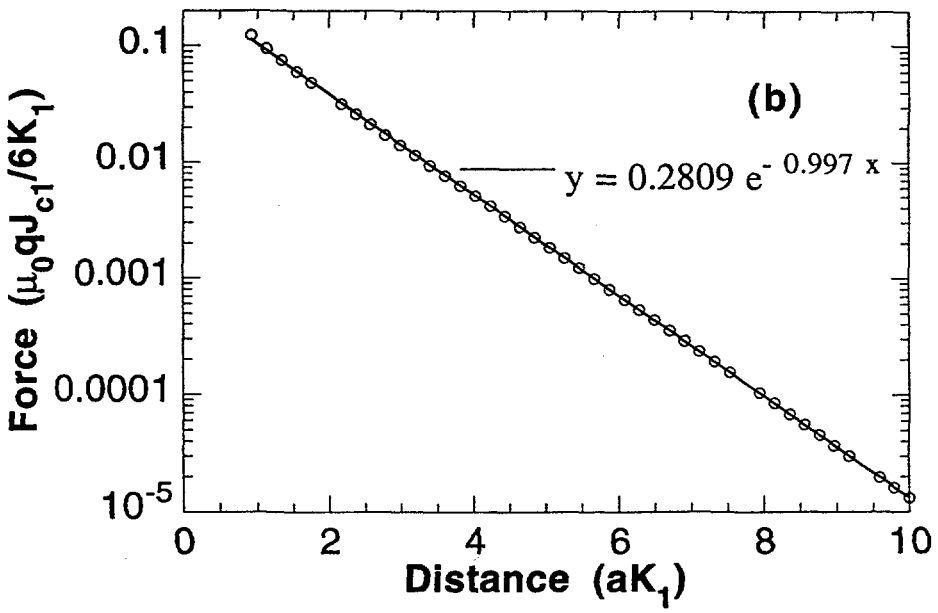

Fig. 6(b) Z. J. Yang

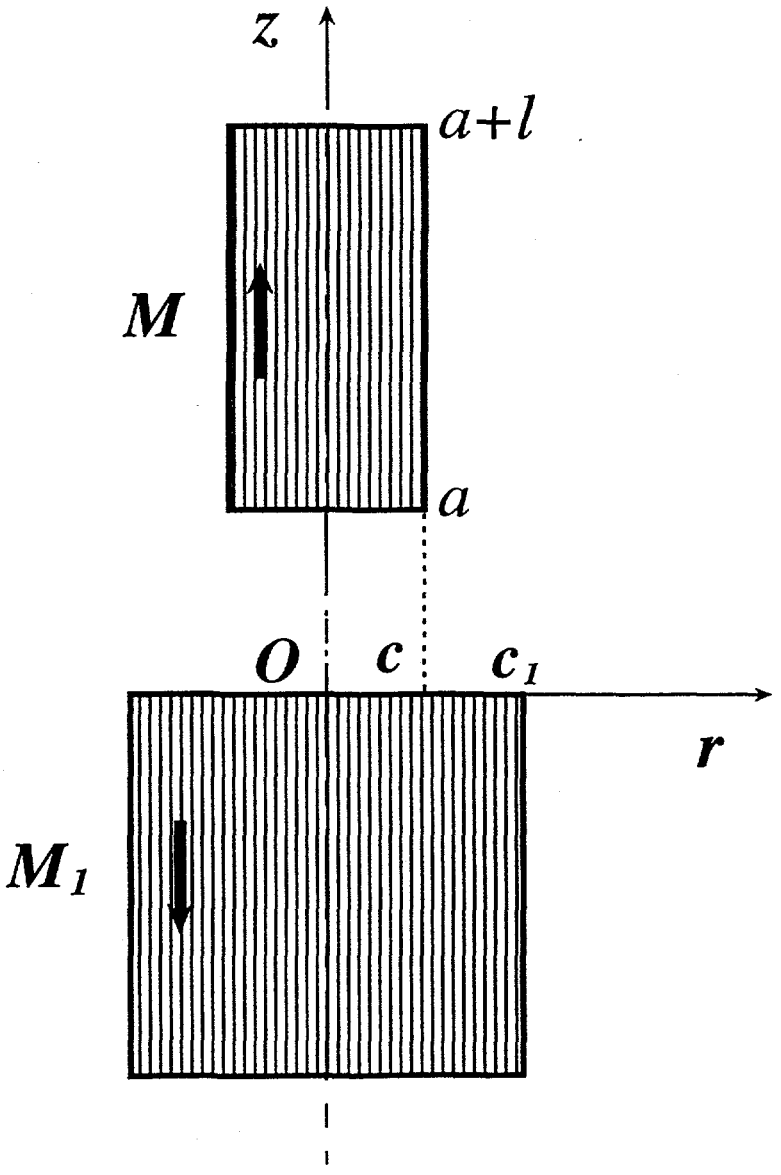

Fig. 7. Z.J. Yang